Structure and Properties of Transition-Metal Complexes with Chiral C_2-Symmetric Binucleating Ligands

by **Christoph J. Fahrni** and **Andreas Pfaltz**[1])*

Institut für Organische Chemie, Universität Basel, St. Johanns-Ring 19, CH-4056 Basel

and **Markus Neuburger** and **Margareta Zehnder***

Institut für Anorganische Chemie, Universität Basel, Spitalstrasse 51, CH-4056 Basel

The coordination behavior of chiral binucleating ligands of type **1**–**4** with various transition metals has been investigated. ^{1}H-NMR Titration experiments with zinc(II) salts gave detailed structural information about the structure of the resulting zinc complexes. Ligand **1** forms an unusual C_3-symmetric dinuclear zinc complex $[Zn_2ClL_3]$ (**8a**) which was characterized by X-ray crystallography. Treatment of complex **8a** with various carboxylic acids resulted in ligand-exchange reactions. With ligand **2**, a hydroxo-bridged dinuclear copper complex **15** was synthesized and its structure elucidated by X-ray analysis. Solution studies UV and ^{1}H-NMR spectroscopy of the reaction of ligand **3** with Zn^{II} and Ni^{II} salts revealed the formation of dimeric species of the type $[M_2X_4L_2]$. Ligand **4** formed well-defined dinuclear complexes with Ni^{II} and Cu^{II} salts of which the corresponding Ni^{II} complex $[Ni_2(AcO)_2(ClO_4)_2L]$ (**22a**) was characterized by crystal-structure analysis.

In the preceding communication [1], we have described the synthesis of chiral binucleating ligands **1**–**4**. Herein, we report on the coordination chemistry of these ligands and the crystal structures of various dinuclear transition-metal complexes.

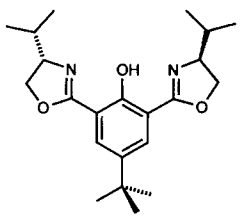

1

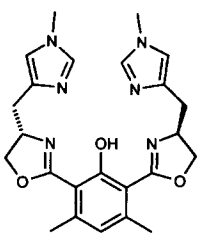

2

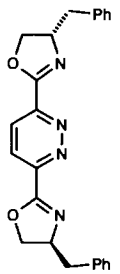

3

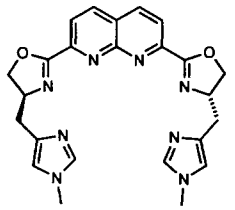

4

1. NMR Studies of Zinc-Complex Formation with Ligand 1. – To investigate the coordination behavior toward zinc ions, portions of $ZnCl_2$ were added successively to a CD_3CN solution of ligand **1** (*Fig. 1*). In the presence of 0.5 mol-equiv. of $ZnCl_2$, extensive broadening of the ^{1}H-NMR signals indicated rapid ligand exchange. At 1.0 equiv. of $ZnCl_2$, a well-resolved spectrum was observed which did not change when the Zn/lig-

[1]) New address: Max-Planck-Institut für Kohlenforschung, Kaiser-Wilhelm-Platz 1, D-45470 Mülheim an der Ruhr.

and ratio was increased to 3:1. Conclusively, only a 1:1 complex is formed under these conditions. The splitting of the *s* at 7.8 ppm corresponding to the two protons of the aromatic ring into two *s* upon complexation with $ZnCl_2$ as well as the splitting of the two *d* of Me_2CH at 1.0 ppm indicated the formation of an unsymmetric complex **5** (*Scheme 1*). This structure was additionally supported by the presence of the proton signal of the phenolic OH group at 12.5 ppm. In a preparative experiment, ligand **1** was complexed with equimolar amounts of $ZnCl_2$ in MeCN. Evaporation of the solvent and crystallization from CH_2Cl_2/hexane afforded complex **5** in 85% yield as pale-yellow needles. The NMR spectrum of this compound in CD_3CN was identical with the spectrum observed upon addition of 1 equiv. of $ZnCl_2$ in the NMR titration experiments. Structure **5** was fully supported by the analytical data including MS and elemental analysis.

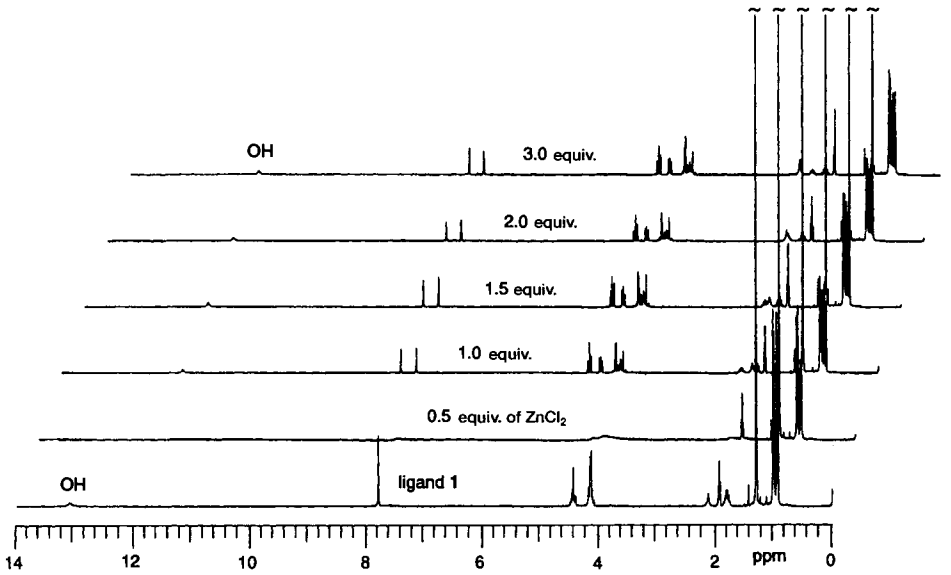

Fig. 1. *^{1}H-NMR Spectra of the titration of ligand* **1** *with $ZnCl_2$ in CD_3CN*

In contrast, treatment of the sodium salt **7** of ligand **1** with $ZnCl_2$ in CD_3CN led to a different product (*Fig. 2*). Addition of 0.5 equiv. of $ZnCl_2$ resulted in a well-resolved spectrum with sharp signals in which the two *d* of Me_2CH were shifted substantially upfield to 0.2 and 0.8 ppm, whereas the remaining signals were shifted downfield. In contrast to complex **5**, the signals of the aromatic protons and the Me_2CH groups indicated that the C_2 symmetry of the ligand was retained in the complex. Successive addition of $ZnCl_2$ up to 3 mol-equiv. resulted in complete conversion to a new complex. The presence of two *tert*-butyl signals implied a structure comprising two ligand molecules in a different coordination environment. Attempts to isolate this complex failed and, therefore, we could not determine its structure.

However, the structure of the complex formed after addition of 0.5 equiv. of $ZnCl_2$ could be elucidated by X-ray analysis. Suitable crystals were obtained from a NMR

Scheme 1

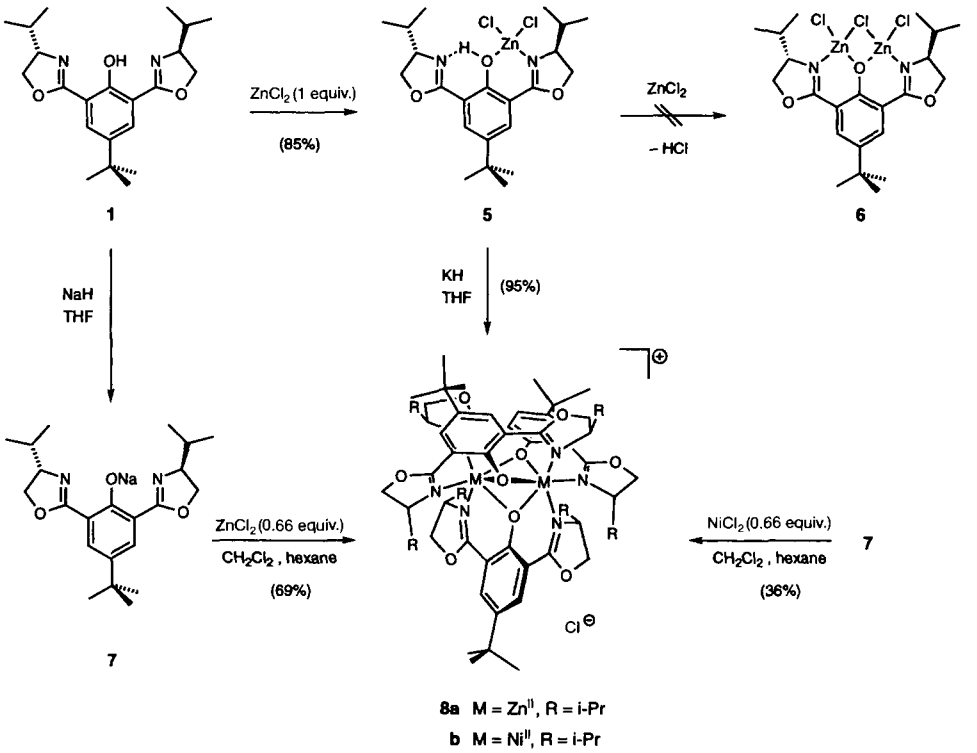

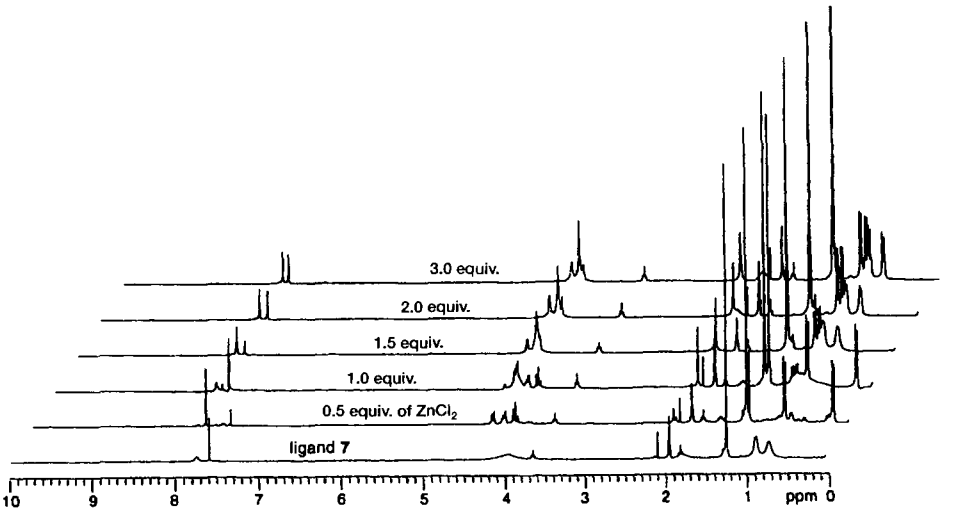

Fig. 2. *^{1}H-NMR Spectra of the titration of the deprotonated ligand* **1** (sodium salt **7**) *with $ZnCl_2$ in CD_3CN*

sample in CD_3CN by slow evaporation over several days. To our surprise, the structure showed a C_3-symmetric arrangement of three ligands coordinated to two Zn cations as depicted in *Scheme 1*. An independent synthesis using sodium salt **7** and $ZnCl_2$ in the correct ratio of 3:2 in refluxing CH_2Cl_2 afforded the crystalline complex **8a** in 69% yield. The NMR spectrum of this compound was identical with that previously observed during the titration experiment. Several attempts to synthesize the dinuclear zinc complex **6** comprising only one ligand failed. After deprotonation of **5** with potassium hydride, complex **8a** was isolated in almost quantitative yield (based on metal). Starting from nickel dichloride hexahydrate, an analogous dinuclear nickel complex **8b** could be obtained, although only in 36% yield. The complex crystallized in two different forms, needles and prisms, which, according to the elemental analysis, differed primarily in the content of crystallization solvent. The mass spectra of both modifications were identical showing isotope intensity distributions consistent with the cations $[Ni_2L_3]^+$ and $[Ni_2L_2]^+$. The prisms, although nice looking, proved to be twinned and, therefore, were not suitable for X-ray analysis.

2. Ligand-Exchange Reactions with Complex 8a. – Treatment of the dinuclear zinc complex **8a** with various carboxylic acids resulted in ligand-exchange reactions which were monitored by NMR and UV spectroscopy. Of particular interest was the question whether there is a preference towards binding of one enantiomer using a chiral carboxylic acid. Hence, a solution of complex **8a** in $CDCl_3$ was titrated with racemic α-methoxybenzeneacetic acid and analyzed by ^{1}H-NMR spectroscopy (*Fig. 3*). In the presence of 0.5 and 1.0 mol-equiv. of acid, the *s* of the MeO protons (3.4 ppm) were shifted apart by 0.25 ppm. The occurrence of two new *d* at 0.9 and 1.0 ppm (Me_2CH), a *s* at 1.3 ppm (*t*-Bu) as well as a broad signal around 12.5 ppm (phenol OH, not shown in *Fig. 3*) indicated the presence of 0.5 and 1.0 mol-equiv. of ligand **1**, respectively. With further increasing acid concentration, the difference in chemical shift gradually decreased, suggesting a dynamic equilibrium between free acid and the formed complexes. An analogously performed UV titration experiment revealed an unexpected complexity of the involved equilibriums which prevented us from determining the binding constants of the two enantiomers (see *Fig. 4,a*, for a typical UV titration experiment). To a solution of complex **8a** in $CHCl_3$, successively a 100-fold more concentrated solution of (*R*)- or (*S*)- α-methoxybenzeneacetic acid was added. After addition of 2 equiv. of carboxylic acid, a clear isosbestic point at 382 nm could be observed when the acid concentration was increased up to 20 equiv., indicating an equilibrium which presumably involves only two different UV-active species. Furthermore, the increasing absorption intensity with a maximum at 336 nm confirmed the release of neutral ligand **1**, in accordance with the NMR titration experiment. A quantitative analysis of the data remains difficult since the isosbestic point could be observed only upon addition of 2 equiv. of carboxylic acid and, therefore, more than one equilibrium system must be involved. A qualitative comparision of the absorption changes at 372 nm *vs.* concentration of added carboxylic acid (*Fig. 4,b*) strongly suggested that the stability constants of the diastereoisomeric complexes derived from (*R*)- and (*S*)-α-methoxybenzene acetate do not differ substantially.

3. Crystal Structure of Complex 8a. – Crystals of the dinuclear zinc complex **8a**, grown in CD_3CN, were found to be cubic with the space group $I2_13$ ($Z = 8$). A detailed

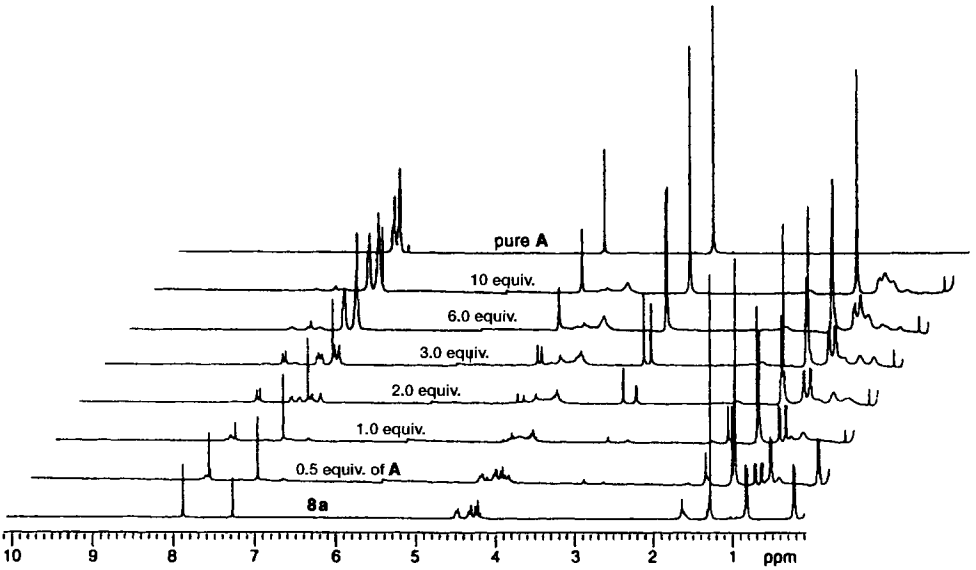

Fig. 3. *^{1}H-NMR Spectra of the titration of complex* **8a** *with racemic α-methoxybenzeneacetic acid* (**A**) *in* $CDCl_3$

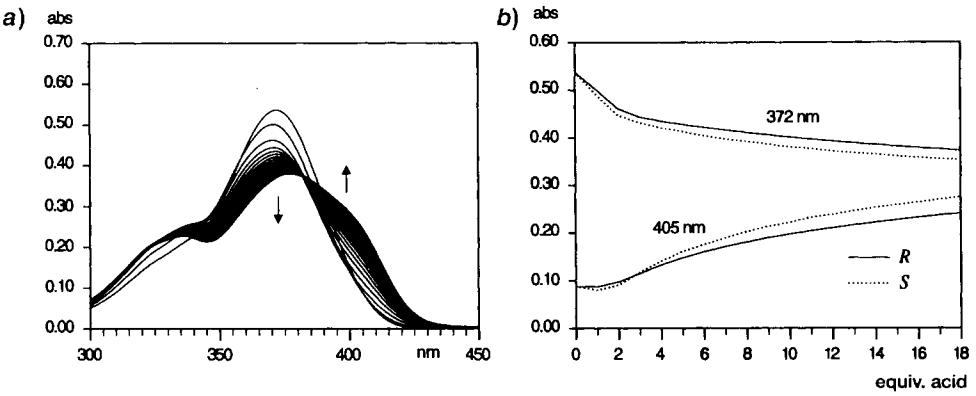

Fig. 4. *Titration of complex* **8a** *with α-methoxybenzeneacetic acid in* $CHCl_3$: a) *UV spectra upon addition of (*R*)-α-methoxybenzeneacetic acid to a 20* μM *solution of* **8a** *in* $CHCl_3$ (0.2 mol-equiv. aliquots); b) *change of absorption at 372 and 405 nm as a function of the concentration of the (*R*)- and (*S*)-enantiomer*

list of the crystal data and data collection parameters is given in *Table 4* (see *Exper. Part*). The asymmetric unit contains two non-identical dinuclear complexes with very similar structural geometries, which are located on the crystallographic C_3 axis together with the two Cl-atoms. An ORTEP plot and a stereoscopic representation of one of the two dinuclear complexes is shown in *Fig. 5*. The two Zn-atoms are surrounded by three ligands in a C_3-symmetric arrangement and are bridged by three phenolato O-atoms. This arrangement results in a distorted octahedral coordination environment of the two metal centers. One of the Zn-atoms forms planar chelate rings with the three ligands and

is located at the intersection of the three ligand planes defined by the aromatic rings. The chelate rings involving the second Zn-atom deviate significantly from planarity. The N–Zn–O plane and the ligand plane form an angle of 41°, with the Zn-atom at a distance of 1.2 Å above the ligand plane (for selected bond lengths and angles, see

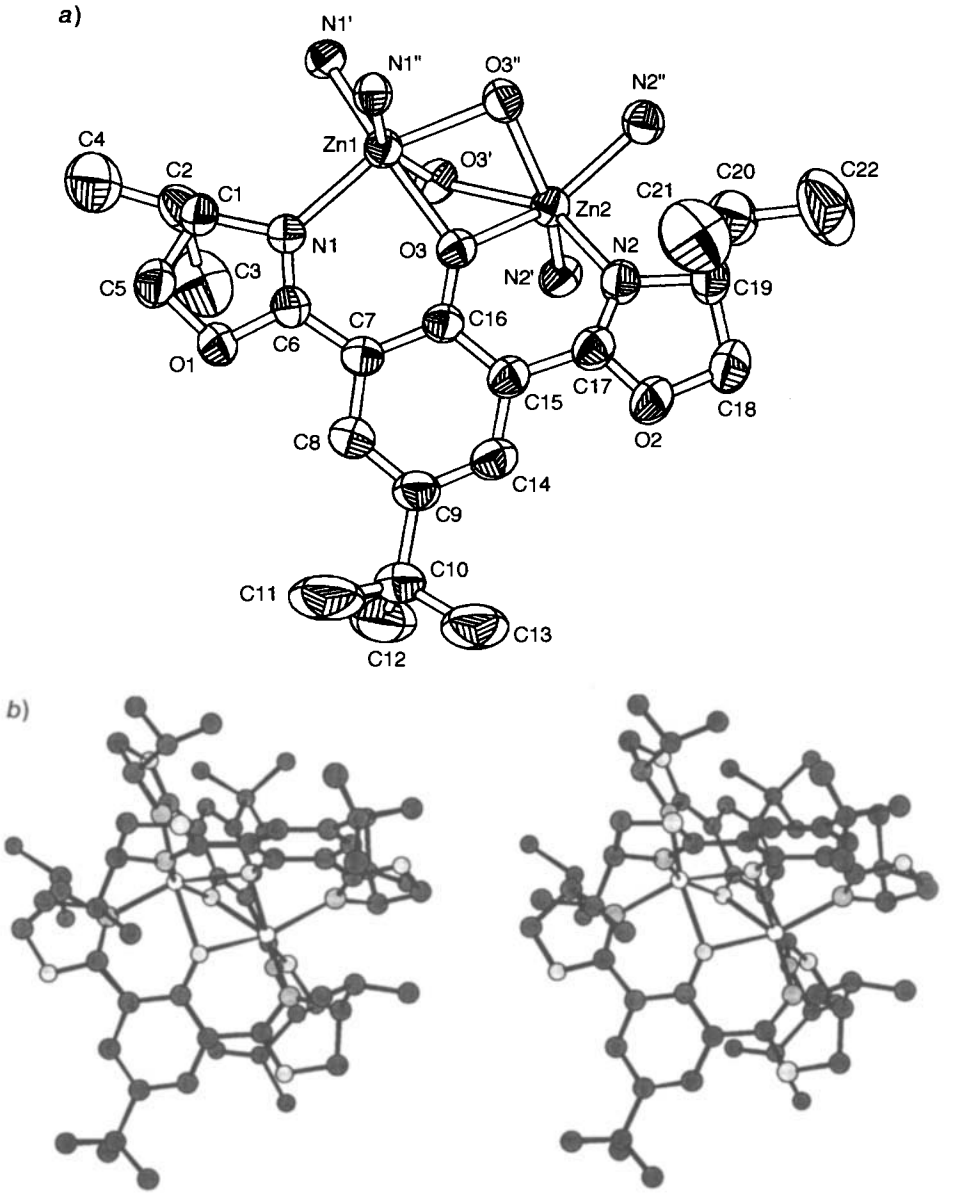

Fig. 5. *Structure of complex* **8a**. a) *ORTEP Plot at the 50% probability level with numbering scheme showing the coordination geometry of the zinc centers* (for clarity, only one of the three coordinating ligands is shown, H-atoms are omitted); b) *stereoscopic view showing one of the two dinuclear cations of the unit cell.* Arbitrary numbering.

Table 1). In contrast, the ^{1}H-NMR spectrum of **8a** shows only one set of signals for the two Me_2CH groups, suggesting equivalent coordination environments of the two Zn-atoms within the NMR time scale due to a rapid interconversion between two conformers with exchanged coordination geometries of the two Zn-centers. The non-bonding Zn···Zn distances in the two complexes are 3.04 and 3.06 Å, respectively.

Table 1. *Selected Bond Lengths* [Å] *and Angles* [deg] *for Complex* **8a**

	Cation *1*	Cation *2*		Cation *1*	Cation *2*
Zn(1)···Zn(2)	3.043(1)	3.056(1)	Zn(2)–O(3)	2.157(2)	2.093(3)
Zn(1)–N(1)	2.117(3)	2.131(3)	Zn(2)–N(2)	2.127(3)	2.104(3)
Zn(1)–O(3)	2.117(2)	2.117(3)			
N(1)–Zn(1)–N(1′)	99.93(9)	100.1(1)	N(2)–Zn(2)–N(2′)	97.4(1)	100.7(1)
N(1)–Zn(1)–N(1″)	99.93(9)	100.1(1)	N(2)–Zn(2)–N(2″)	97.4(1)	100.7(1)
N(1)–Zn(1)–O(3)	83.2(1)	80.4(1)	O(3)–Zn(2)–N(2)	79.2(1)	81.9(1)
N(1)–Zn(1)–O(3′)	101.1(1)	107.8(1)	O(3)–Zn(2)–N(2)	113.8(1)	103.0(1)
N(1)–Zn(1)–O(3″)	158.9(1)	151.7(1)	O(3)–Zn(2)–N(2″)	148.8(1)	155.3(1)
O(3)–Zn(1)–O(3′)	75.7(1)	72.6(1)	O(3)–Zn(2)–O(3′)	74.06(9)	73.6(1)
O(3)–Zn(1)–O(3″)	75.7(1)	72.6(1)	O(3)–Zn(2)–O(3″)	74.06(9)	73.6(1)
Zn(1)–O(3)–Zn(2)	90.82(9)	93.1(1)			

Whereas several dinuclear zinc complexes were reported with two hydroxo or alkoxo bridges (*Fig. 6*), complex **8a** represents the first example of a dinuclear zinc complex with *three* O-bridges. The Zn···Zn distance in **8a** is shorter than in the corresponding

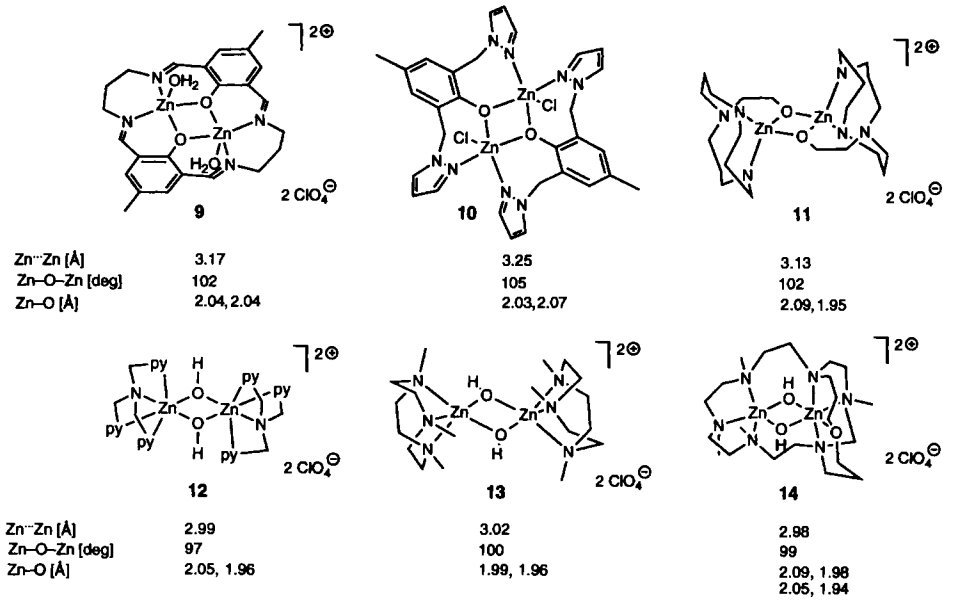

Fig. 6. *Coordination geometries of selected dioxo-bridged dinuclear zinc complexes*

μ-alkoxo-bridged complexes **9** [2], **10** [3], or **11** [4] but similar to the distances found in the μ-hydroxo-bridged complexes **12** [5], **13** [6], or **14** [7]. The Zn–O bond lengths in **8a** are by *ca.* 0.1 Å longer than the average distances in the dioxo-bridged complexes **9**–**14**, whereas the measured Zn–O–Zn angles (90.82(9) and 93.1(1), resp.) are significantly smaller by *ca.* 10°.

4. Crystal Structure of the Dinuclear Copper Complex 15. – Treatment of ligand **2** with 2 equiv. of copper(II) perchlorate hexahydrate in MeOH and slow evaporation of the solvent afforded the dinuclear complex **15** as blue needles in 52% yield (*Scheme 2*). Recrystallization from MeOH/EtOH 10:1 afforded dark blue prisms which were suitable for X-ray analysis.

Scheme 2

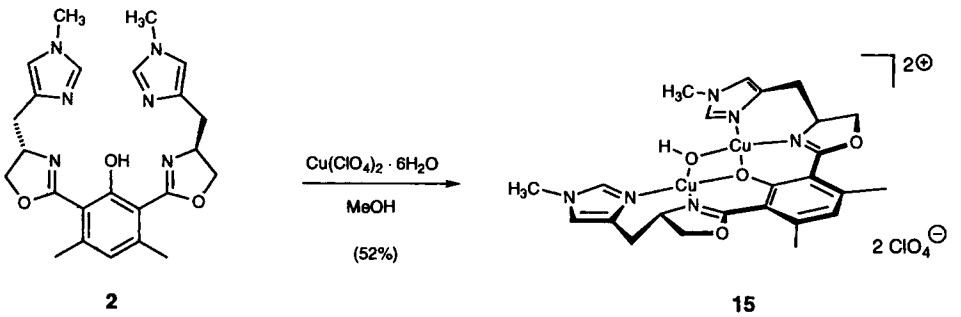

2 **15**

The crystals were found to belong to the triclinic space group *P*1, and each asymmetric unit contains two dinuclear complexes of slightly different geometry, four perchlorate residues, and two molecules of H_2O (for crystal data and data collection parameters, see *Table 4* in the *Exper. Part*). *Fig. 7* displays the structure of one of the two dications, and *Table 2* summarizes selected bond lengths and angles. The two Cu^{II} ions are coordinated to the bidentate dihydrooxazole-imidazole moiety and are bridged by a phenolate and a hydroxy group, adopting a slightly distorted square-planar coordination geometry. A similar geometry is found in numerous achiral (*Schiff* base)dicopper complexes consisting of the same N_4O_2 donor set such as **16** [8], **17** [9], **18** [10], and **19** [11] (*Fig. 8*). The Cu···Cu distances (2.947(1) and 2.943(1)Å) closely match the distances observed in complexes **16**–**19**. The Cu–OH bond lengths in **15** are 1.899(6) and 1.905(6) Å for dication *1* and 1.902(6) and 1.892(6) Å for dication *2*, respectively. The corresponding Cu–OR(phenoxide) bond lengths are slightly longer (1.987(6) and 1.995(6) Å for dication *1* and 2.001(6) and 1.989(6) Å for dication *2*). These values closely match the bond lengths in structures **16**–**19**. Two of the four perchlorate ions serve as weak, unsymmetrically coordinated bridging ligands with significantly different Cu–O distances of 2.57 and 2.82 Å and 2.54 and 2.91 Å, respectively. The four-membered Cu_2O_2 unit deviates from planarity with torsion angles (O(1)–Cu(1)–O(2)–Cu(2)) of 10.2 and 6.7° for dication *1* and dication *2*, respectively. These values are comparable to the torsion angle in the achiral complex **17** (9.3°). Consequently, the deviation seems not to be caused by the two chiral dihydrooxazole moieties. On the contrary, the preferred square-planar coordination geometry of the two Cu^{II} centers affects the ligand geometry by slightly

rotating the two dihydrooxazole rings out of the plane defined by the aryl moiety. The corresponding torsion angles N(3)–C(9)–C(2)–C(1) and N(4)–C(10)–C(6)–C(1) are 12.4 and 6.3° for dication *1* and 8.6 and 6.3° for dication *2*, respectively.

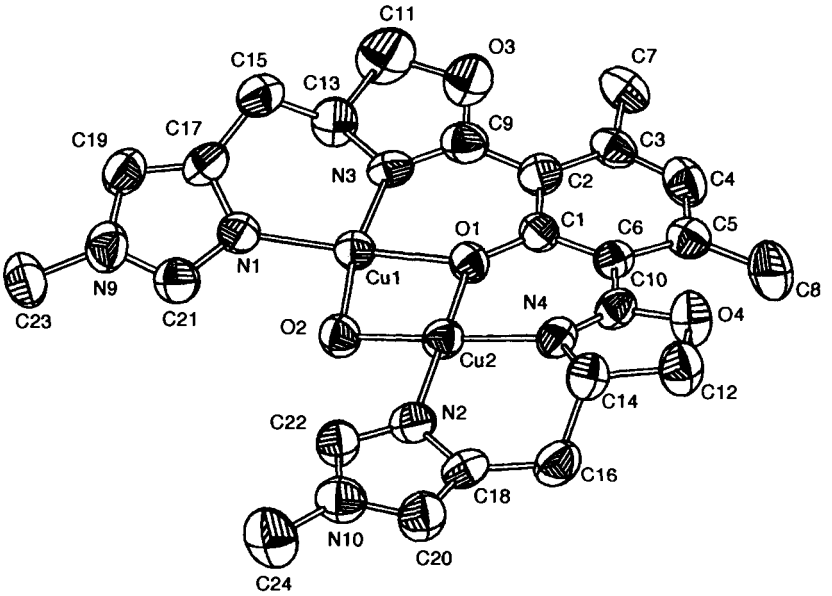

Fig. 7. *ORTEP View of complex* **15** *at the 50% probability level.* Only one of the two dinuclear cations is shown; H-atoms are omitted for clarity; arbitrary numbering.

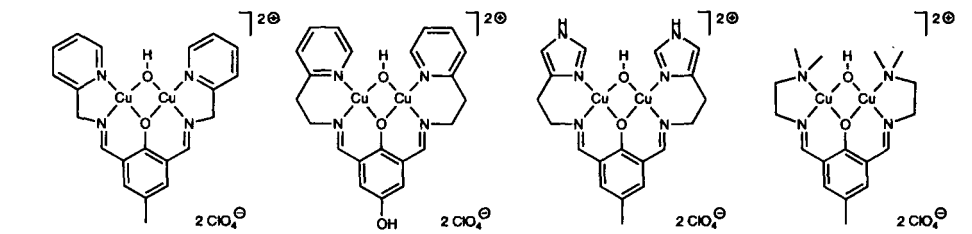

	16	**17**	**18**	**19**
Cu···Cu [Å]	2.94	2.99	3.01	2.92
Cu-OH [Å], Cu-OR [Å]	1.92, 1.93	1.93, 1.96	1.90, 1.96	1.92, 1.95

Fig. 8. *Coordination geometries of selected hydroxo-bridged dinuclear copper complexes with a* N_4O_2 *donor set*

5. NMR and UV Studies of Complex Formation with the Pyridazine Ligand 3. – The complexation behavior of ligand **3** was investigated by NMR and UV titration experiments (*Figs. 9* and *10*). NMR Titration with $ZnCl_2$ was performed as described for ligand **1**. After addition of 0.5 equiv. of the metal salt, a well-resolved spectrum was observed with a downfield shift of most signals, indicating a fast dynamic equilibrium

Table 2. *Selected Bond Lengths* [Å] *and Angles* [deg] *for Complex* **15**

	Dication *1*	Dication *2*		Dication *1*	Dication *2*
Cu(1)···Cu(2)	2.947(1)	2.943(1)			
Cu(1)–O(1)	1.987(6)	2.001(6)	Cu(2)–O(1)	1.995(6)	1.989(6)
Cu(1)–O(2)	1.899(6)	1.902(6)	Cu(2)–O(2)	1.905(6)	1.892(6)
Cu(1)–N(1)	1.963(7)	1.970(8)	Cu(2)–N(2)	1.968(8)	1.981(7)
Cu(1)–N(3)	1.905(7)	1.938(7)	Cu(2)–N(4)	1.909(7)	1.922(7)
O(1)–Cu(1)–O(2)	80.8(2)	80.9(3)	O(1)–Cu(2)–O(2)	80.5(2)	81.5(2)
O(1)–Cu(1)–N(1)	172.9(3)	175.6(3)	O(1)–Cu(2)–N(2)	174.3(3)	176.8(3)
O(2)–Cu(1)–N(1)	96.3(3)	95.5(3)	O(2)–Cu(2)–N(2)	96.2(3)	95.4(3)
N(1)–Cu(1)–N(3)	93.9(3)	95.3(3)	N(2)–Cu(2)–N(4)	94.7(3)	93.2(3)
O(1)–Cu(1)–N(3)	89.3(3)	88.3(3)	O(1)–Cu(2)–N(4)	88.0(3)	89.9(3)
O(2)–Cu(1)–N(3)	169.7(3)	168.7(3)	O(2)–Cu(2)–N(4)	166.6(3)	166.2(3)
Cu(1)–O(1)–Cu(2)	95.5(2)	95.1(3)	Cu(1)–O(2)–Cu(2)	101.5(3)	101.8(3)

between complexed and uncomplexed ligand. The spectrum obtained at a 1:1 metal/ligand ratio was similar, except for additional signal shifts. Subsequently, each addition of $ZnCl_2$, up to 4 equiv., caused only marginal changes, except for the CH_2O *m* of the dihydrooxazole rings at 4.3 ppm which gradually shifted downfield. The data from an analogous UV titration (*Fig. 10, a*) was in agreement with these observations. Two definite isosbestic points at 239 and 292 nm indicated an equilibrium involving onyl two UV-active species in significant concentrations. A similar UV titration with $NiCl_2$ showed the same qualitative behavior (*Fig. 10, b*). These results were consistent with a dimeric species **21** in equilibrium with the free ligand **3** and metal dichloride. The formation of **21** occurred presumably *via* a mononuclear species **20**. However, according to results from the NMR and UV titration experiments, the thermodynamic stability of the dinuclear complex **21** must be much higher, thus resulting in a very low and non-detectable concentration of the mononuclear species **20**.

In agreement with these results, treatment of ligand **3** with 1 equiv. $NiCl_2$ in MeOH afforded the dinuclear complex **21b** in 79% yield. Crystals grown in MeCN over several weeks were used for an X-ray structure analysis. The quality of the crystals only allowed an isotropic refinement of the data up to a final *R* value of 8.48% (monoclinic with space

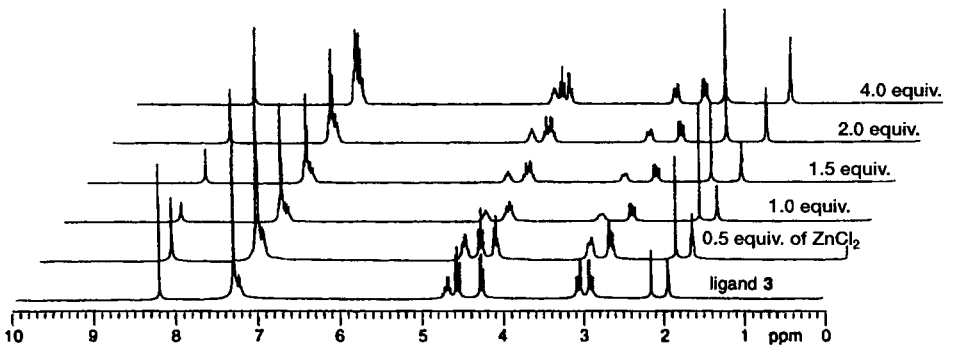

Fig. 9. *^{1}H-NMR Spectra of the titration of ligand* **3** *with $ZnCl_2$ in CD_3CN*

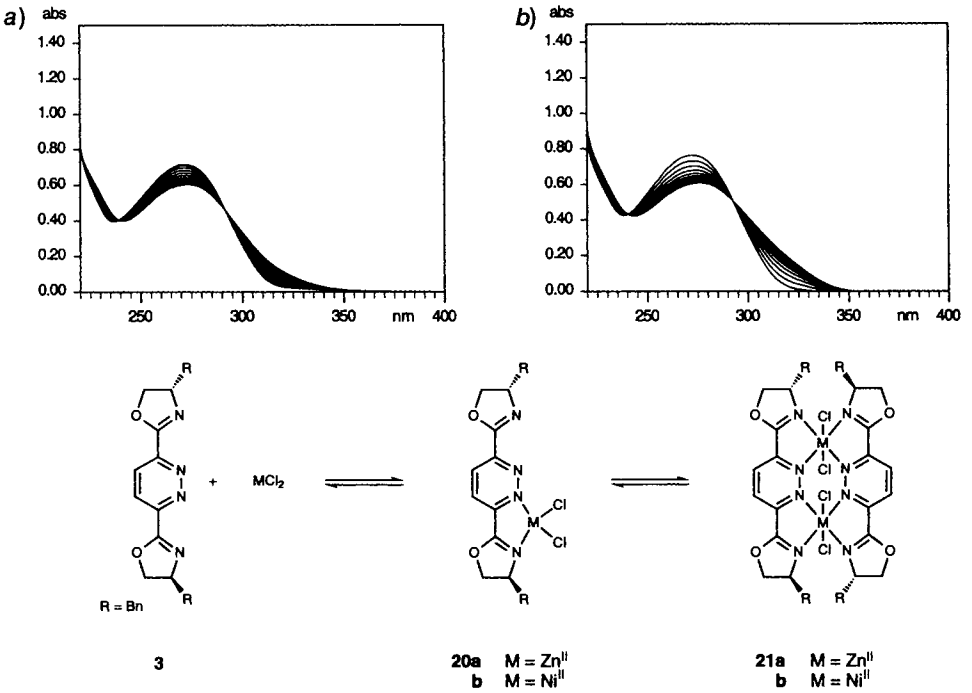

Fig. 10. *UV Spectra of the titration of ligand* **3** (60 μM) *with* a) $ZnCl_2$ *and* b) $NiCl_2$ *in methanol*

group $P2_1$, $a = 8.481$ Å, $b = 31.015$ Å, $c = 10.902$ Å, $\alpha = 90°$, $\beta = 97.739°$, $\gamma = 90°$). Nevertheless, the data unambiguously confirmed structure **21b** with two hexacoordinated Ni-centers. In accordance with the dimeric structure of this complex, the positive-ion FAB mass spectrum showed signal clusters for the fragments $[Ni_2Cl_3L_2]^+$ and $[Ni_2Cl_2L_2]^+$. The ^{1}H-NMR spectrum in CD_3OD exhibited significant line broadening and chemical shifts of up to 18 ppm (*Fig. 11,a*). For a fully paramagnetic Ni^{II} complex, larger paramagnetic shifts and more extensive line broading would be expected. However, the observed spectrum could result from an equilibrium between a diamagnetic complex with two tetracoordinated Ni-centers and minor amounts of a penta- or hexacoordinated paramagnetic complex. The relatively moderate paramagnetic shifts and line widths could also be the consequence of strong antiferromagnetic coupling of two high-spin Ni-centers. Numerous binuclear Ni^{II} complexes with similar ligands derived from phthalazines, pyridazines, pyrazoles, triazoles, and hydrazines are known in which the metal centers are antiferromagnetically coupled *via* a superexchange mechanism [12]. Variable-temperature magnetic studies on the structurally related, pyridazine-bridged binuclear Ni^{II} complex $[Ni_2(ppd)_2(H_2O)_4]Cl_4 \cdot 2\,H_2O$ (ppd = 3,6-bis(1*H*-pyrazol-1-yl)pyridazine) indicated strong coupling with $-J = 14.8\ cm^{-1}$ and an effective magnetic moment μ_{eff} of 2.95 B.M. (room temperature) [12].

After treatment of complex **21b** with excess silver trifluoromethanesulfonate (AgOTf) in CD_3OD, a well-resolved spectrum was obtained (*Fig. 11,b*). Obviously, the resulting complex with non-coordinating triflate counterions is diamagnetic and contains two square-planar Ni^{II} centers, even in a nucleophilic solvent like MeOH.

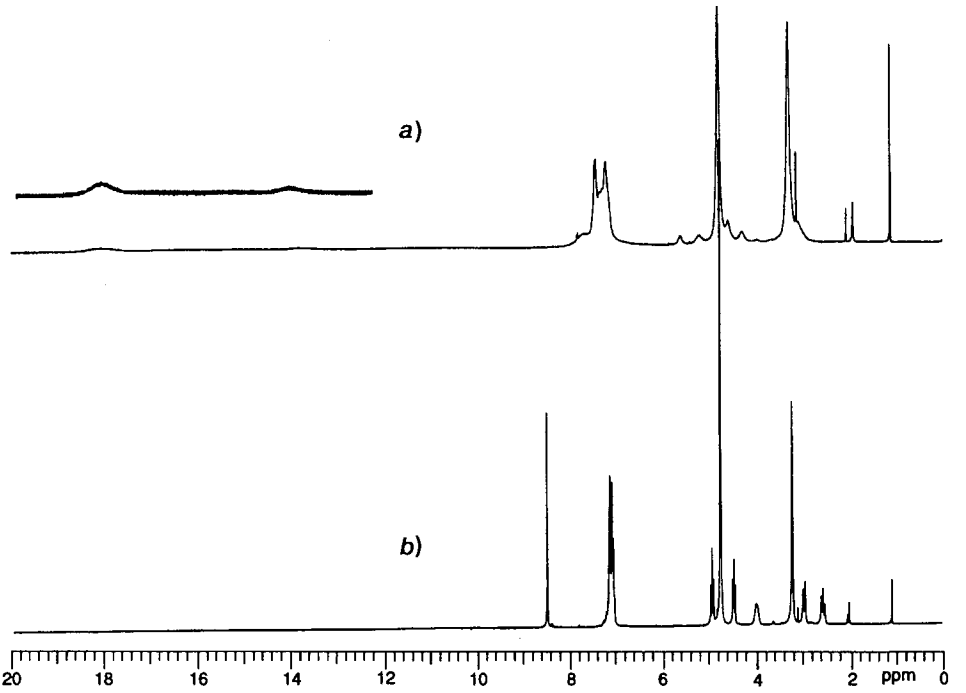

Fig. 11. a) *^{1}H-NMR Spectrum of complex* **21b** *in CD_3OD.* b) *Spectrum after ligand exchange with AgOTf*

6. Dinuclear Transition-Metal Complexes with Ligand 4. – With ligand **4**, the synthesis of crystalline copper and nickel complexes was accomplished. The ligand was treated with a MeOH solution of the corresponding metal acetate followed by a concentrated aqueous solution of sodium perchlorate to afford the crystalline dinuclear complexes **22a** and **22b** after standing for several days (*Scheme 3*). The copper complex **22b** was isolated as thin needles which were not suitable for X-ray analysis. However, the crystals obtained from nickel(II) acetate and ligand **4** (77% yield) were of sufficient quality for a crystal-

Scheme 3

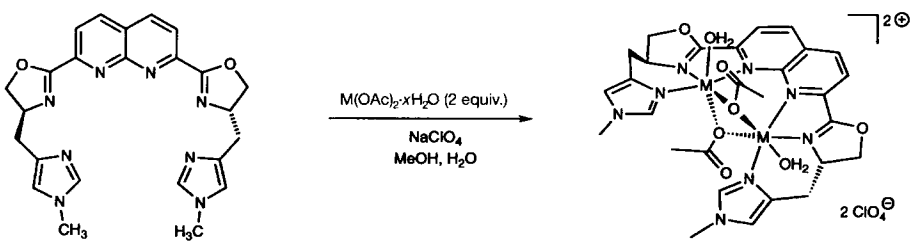

4

22a M = Ni^{II} $[Ni_2(AcO)_2(ClO_4)_2(H_2O)_2L]$

b M = Cu^{II} $[Cu_2(ClO_4)_4(H_2O)_4L]$, *i.e.* Formula without 2 AcO

structure determination. They were orthorhombic belonging to the space group $P2_12_12_1$. The unit cell consists of four identical dinuclear complexes (for crystal data and data collection parameters, see *Table 4* in the *Exper. Part*).

The asymmetric unit of the structure of **22a** contains the dication $[Ni_2(AcO)_2(LH_2O)_2]^{2+}$, which is shown in *Fig. 12*, two perchlorate ions located outside of the coordination sphere, and one molecule of MeOH. The two Ni-centers are held in a strongly distorted octahedral coordination geometry and are bridged by two C_2-symmetrically arranged acetate anions. Additionally, each metal center is coordinated by one H_2O molecule. The relatively short O–O distances (2.56 and 2.57 Å) of the water O-atoms to the adjacent carbonyl groups of the coordinated acetates suggests the presence of a H-bond. The Ni···Ni distance is 3.132(1) Å and thus 0.86 Å longer than the distance of the two naphthyridine N-atoms N(1) and N(2). Both metal centers are twisted C_2-symmetrically out of the plane of the naphthyridine moiety by an angle of 16°. The planes defined by C(1)–N(1)–Ni(1) and C(8)–N(2)–Ni(2) form an angle of 29°, and the distances of the Ni-centers to the naphthyridine plane are 0.64 Å each. In contrast to the structure of complex **15**, the π-systems of the two dihydrooxazole rings are

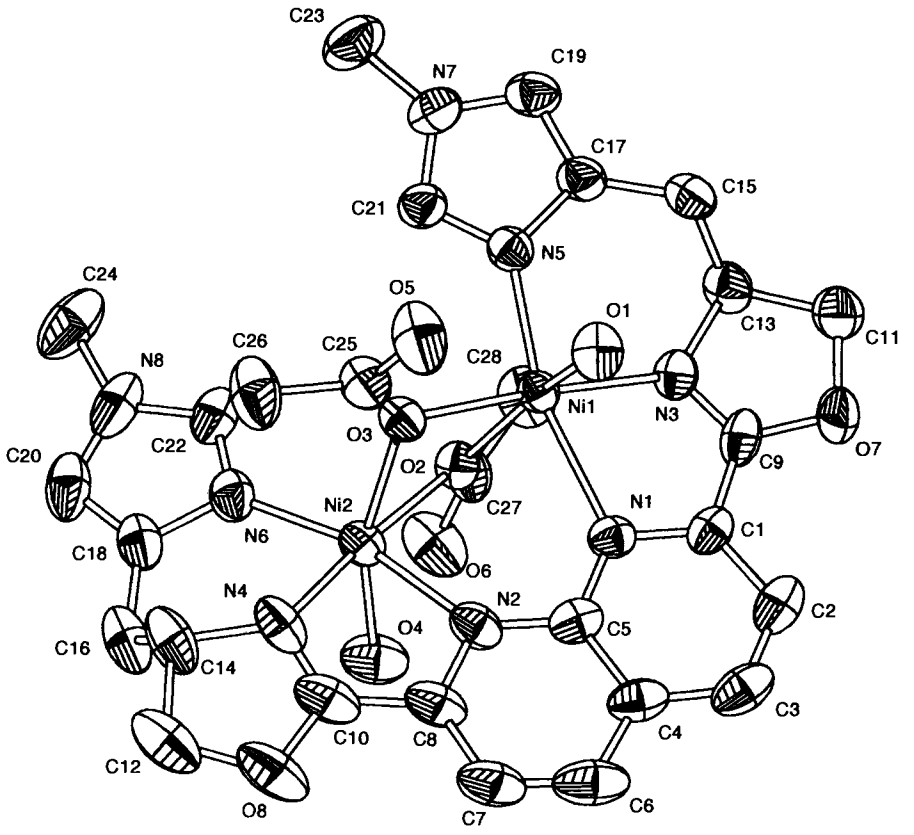

Fig. 12. *ORTEP Representation at the 50% probability level of complex* **22a** *showing the dinuclear dication.* H-Atoms are omitted for clarity, arbitrary numbering.

essentially coplanar with the naphthyridine system (the corresponding dihedral angles C(7)–C(8)–C(10)–N(4) and C(2)–C(1)–C(9)–N(3) are 179.8° and 180.0°, respectively; for selected bond lengths and bond angles, see *Table 3*).

Table 3. *Selected Bond Lengths* [Å] *and Angles* [deg] *for Complex* **22a**

Ni(1)···Ni(2)	3.132(1)	Ni(1)–O(2)	2.079(4)	Ni(2)–N(6)	2.029(5)
Ni(1)–N(1)	2.233(5)	Ni(1)–O(3)	2.078(4)	Ni(2)–O(2)	2.079(4)
Ni(1)–N(3)	2.017(5)	Ni(2)–N(2)	2.205(6)	Ni(2)–O(3)	2.100(4)
Ni(1)–N(5)	2.035(5)	Ni(2)–N(4)	2.054(5)	Ni(2)–O(4)	2.052(5)
Ni(1)–O(1)	2.091(4)				
N(1)–Ni(1)–N(3)	75.6(2)	N(5)–Ni(1)–O(3)	101.8(2)	N(4)–Ni(2)–O(3)	174.3(2)
N(1)–Ni(1)–N(5)	164.1(2)	O(1)–Ni(1)–O(2)	88.8(2)	N(4)–Ni(2)–O(4)	93.9(2)
N(1)–Ni(1)–O(1)	86.3(2)	O(1)–Ni(1)–O(3)	161.2(2)	N(6)–Ni(2)–O(2)	99.5(2)
N(1)–Ni(1)–O(2)	99.8(2)	O(2)–Ni(1)–O(3)	76.6(1)	N(6)–Ni(2)–O(3)	96.7(2)
N(1)–Ni(1)–O(3)	84.6(2)	N(2)–Ni(2)–N(4)	75.5(2)	N(6)–Ni(2)–O(4)	93.5(2)
N(3)–Ni(1)–N(5)	88.6(2)	N(2)–Ni(2)–N(6)	164.0(2)	O(2)–Ni(2)–O(3)	76.1(2)
N(3)–Ni(1)–O(1)	88.5(2)	N(2)–Ni(2)–O(2)	87.6(2)	O(2)–Ni(2)–O(4)	159.3(2)
N(3)–Ni(1)–O(2)	174.8(2)	N(2)–Ni(2)–O(3)	98.9(2)	O(3)–Ni(2)–O(4)	86.6(2)
N(3)–Ni(1)–O(3)	105.1(2)	N(2)–Ni(2)–O(4)	84.0(2)	Ni(1)–O(2)–Ni(2)	97.8(2)
N(5)–Ni(1)–O(1)	91.2(2)	N(4)–Ni(2)–N(6)	89.0(2)	Ni(1)–O(3)–Ni(2)	97.1(2)
N(5)–Ni(1)–O(2)	95.9(2)	N(4)–Ni(2)–O(2)	102.3(2)		

Coordination of ligand **4** with $Cu(OAc)_2$ under the same conditions previously used for the preparation of the nickel complex **22a** led to a different type of complex. Analysis of the mass and IR spectra of the isolated copper complex **22b** revealed a structure lacking any acetate ligands. In the region of 1570 to 1575 cm^{-1} of the IR spectrum, no resonance was observed which could be assigned to the C=O vibration of an acetate. In the mass spectrum, no cluster was detected with an isotope distribution corresponding to a fragment containing an acetate residue. In contrast to these findings, the mass spectrum of the Ni-complex **22a** showed among other signals two clusters for the fragments $[Ni_2(AcO)_2L]^+$ and $[Ni_2(AcO)_2(ClO_4)L]^+$. According to the elemental analysis, compound **22b** contained four perchlorate ions and, therefore, no acetates can be present. A detailed analysis of the IR spectrum in the regions 1000–1200 cm^{-1} and 600–650 cm^{-1} led to the conclusion that one or two of the perchlorate ions is coordinated to the Cu-centers. Three intense vibrations at 1089, 1114, and 1144 cm^{-1} were observed, consistent with the expected C_2 symmetry of a coordinated, bridging perchlorate [13].

7. Conclusion. – Our results demonstrate that chiral C_2-symmetric dihydrooxazole ligands **1**–**4** readily form various types of binuclear Ni^{II}, Cu^{II}, and Zn^{II} complexes. Complexes of this kind are of interest as potential catalysts for enantioselective transformations. Preliminary experiments have shown that copper complexes derived from bis(dihydrooxazoles) **1**–**4** and related ligands catalyze allylic oxidations of olefins with peroxy esters. The results of these studies will be reported in due course.

Financial support of this work by the *Swiss National Science Foundation* is gratefully acknowledged.

Experimental Part

General. See [1]. Solvents and reagents: MeCN, CH_2Cl_2, MeOH, EtOH, THF: *Fluka puriss.*; sodium hydride: *Fluka pract.*; $ZnCl_2$, $Zn(OAc)_2 \cdot 2\,H_2O$, $NiCl_2 \cdot 6\,H_2O$, $Ni(OAc)_2 \cdot 4\,H_2O$, $Cu(OAc)_2 \cdot H_2O$, $Cu(ClO_4)_2 \cdot 6\,H_2O$, $NaClO_4 \cdot H_2O$, AgOTf: *Fluka purum.* Syntheses of ligands **1**–**4**: see [1].

*{4-(*tert*-Butyl)-2-[(4S)-4,5-dihydro-4-isopropyloxazol-2-yl-κN³]-6-[(4S)-4,5-dihydro-4-isopropyloxazol-2-yl]phenol-κO}zinc Dichloride* (**5**). Ligand **1** (100 mg, 0.268 mmol) was added to a soln. of anh. $ZnCl_2$ (36 mg, 0.27 mmol) in MeCN (5 ml). After stirring for 10 min at r.t., the resulting homogeneous yellow soln. was evaporated and the residue dissolved in CH_2Cl_2 (3 ml). The soln. was subsequently covered with a layer of hexane (5 ml) and allowed to stand at r.t. overnight. The crystallized product was filtered, washed with hexane, and dried *in vacuo* to afford 120 mg (85%) of **5**. Pale yellow cotton-like solid. M.p. 285–290° (dec.). $[\alpha]_D = +167.6$ ($c = 0.31$, $CHCl_3$). UV ($CHCl_3$): 392 (11100), 251 (14000). IR (KBr): 3515*m* (br.), 3187*w* (br.), 2962*s*, 2873*m*, 1646*s*, 1613*s*, 1593*m*, 1542*s*, 1464*m*, 1440*m*, 1385*m*, 1365*m*, 1319*w*, 1272*s*, 1172*m*, 1103*m*, 1052*w*, 1026*w*, 988*m*, 928*w*, 839*w*, 796*m*, 737*w*, 608*w*. ^{1}H-NMR ($CDCl_3$, 300 MHz): 0.95 (*d*, $J = 6.7$, Me_2CH); 1.01 (*d*, $J = 5.7$, Me_2CH); 1.09 (*d*, $J = 5.5$, Me_2CH); 2.03 (*d*, $J = 6.7$, Me_2CH); 1.29 (*s*, *t*-Bu); 2.02–2.11 (*m*, Me_2CH); 2.46–2.53 (*m*, Me_2CH); 4.33 (*t*, $J = 8.2$, CH_2O); 4.41–4.48 (*m*, CH_2O, $CHCH_2O$); 4.55–4.70 (*m*, CH_2O, $CHCH_2O$); 4.95 (*t*, $J = 9.6$, CH_2O); 7.84 (*d*, $J = 2.8$, arom. H); 8.17 (*d*, $J = 2.6$, arom. H); 12.45 (br. *s*, OH). ^{13}C-NMR ($CDCl_3$, 75 MHz): 15.3, 17.3, 17.8, 18.9 (Me_2CH); 30.2, 31.8 (Me_2CH); 31.0 (Me_3C); 34.0 (Me_3C); 63.2, 69.7 (CHN); 67.4, 73.1 (CH_2O); 107.1, 113.6 (C(2), C(6)); 131.9, 138.6 (C(3), C(5)); 137.4 (C(4)); 165.8 (C(1)); 169.4, 170.9 (C=N). FAB-MS (NBA): isotope cluster for $[ZnCl L]^+$ (obs., calc.): 478 (3.0, 3.8), 477 (15.3, 16.5), 476 (16.4, 18.2), 475 (59.0, 62.7), 474 (32.5, 32.1), 473 (93.0, 93.2) 472 (28.6, 26.0), 471 (100, 100); cluster for $[L + H]^+$: 375 (3.2, 2.6), 374 (23.0, 23.7), 373 (94.3, 94.0); 547 (10), 427 (5), 329 (19), 288 (28), 202 (23), 103 (8), 57 (13). Anal. calc. for $C_{22}H_{32}Cl_2N_2O_3Zn \cdot H_2O$: C 50.58, H 6.27, N 5.35; found: C 50.16, H 6.51, N 5.35.

*Tris{μ-{4-(*tert*-butyl)-2,6-{bis[(4S)-4,5-dihydro-4-isopropyloxazol-2-yl]-1κN³,2κN³}phenolato-1:2 κ²O}}dizinc(II) Chloride* (**8a**). A mixture of ligand **1** (200 mg, 0.53 mmol) and NaH (19.3 mg, 0.80 mmol) in anh. THF (5 ml) was refluxed for 30 min. After cooling to r.t., the soln. was filtered (wad of cotton wool in a pipette), evaporated, and dried *in vacuo* affording 207 mg (98%) of **7** as a glassy solid. A mixture of **7** (207 mg, 0.52 mmol) and 49 mg (0.35 mmol) of anh. $ZnCl_2$ in CH_2Cl_2 (4 ml) was refluxed for 30 min with vigorous stirring. After cooling to r.t., the soln. was filtered, the filtrate evaporated, and the residue dissolved in CH_2Cl_2 (2 ml). The soln. was transferred into a 10-ml vial and covered with a layer of hexane (6 ml), the vessel sealed, and the mixture allowed to stand at r.t. for 24 h. The crystalline product was filtered off, washed with hexane and dried *in vacuo*: 155 mg (69%) of **8a**. Pale yellow needles. M.p. 300–305°. $[\alpha]_D = +1144.5$ ($c = 0.16$, $CHCl_3$). UV (MeOH): 372 (23900), 252 (35900), 217 (107400). IR (KBr): 3425*m* (br.), 2961*s*, 2904*m*, 2871*m*, 1632*s*, 1599*m*, 1578*m*, 1556*m*, 1481*m*, 1461*m*, 1368*m*, 1329*w*, 1300*w*, 1267*m*, 1251*m*, 1215*m*, 1186*s*, 1083*m*, 1050*w*, 1003*m*, 977*m*, 905*w*, 842*w*, 795*m*, 740*w*, 612*w*, 534*w*, 478*w*. ^{1}H-NMR (CD_3CN, 300 MHz): 0.19 (*d*, $J = 6.8$, Me_2CH); 0.78 (*d*, $J = 7.1$, Me_2CH); 1.26 (*s*, *t*-Bu); 1.56–1.62 (*m*, Me_2CH); 4.14 (*t*, $J = 9.1$, 1 H, CH_2O); 4.28 (*dt*, $J = 9.1$, 3.1, $CHCH_2O$); 4.42 (*dd*, $J = 9.1$, 3.3, 1 H, CH_2O); 7.91 (*s*, arom. H). ^{13}C-NMR (CD_3CN, 75 MHz): 13.2, 18.7 (Me_2CH); 31.4 (Me_2CH); 31.6 (Me_3C); 34.5 (Me_3C); 66.8 (CH_2O); 70.6 (CHN); 113.5 (C(2), C(6)); 133.7 (C(3), C(6)); 136.1 (C(4)); 167.0 (C(1)); 168.7 (C=N). FAB-MS: isotope cluster for $[Zn_2L_3]^+$ (obs., calc.): 1251 (3.0, 4.9), 1250 (11.3, 12.3), 1249 (22.2, 24.5), 1248 (33.5, 35.4), 1247 (56.1, 58.1), 1246 (69.0, 69.0), 1245 (97.3, 100), 1244 (80.6, 71.3), 1243 (100, 90.5), 1242 (60.3, 48.2), 1241 (73.4, 61.7); cluster for $[Zn_2L_2]^+$: 878 (2.5, 3.3), 877 (4.6, 4.5), 876 (4.6, 5.2), 875 (7.6, 5.2), 874 (8.5, 7.9), 873 (12.0, 12.6), 872 (9.2, 8.4), 871 (12.6, 12.1), 870 (6.1, 6.3), 869 (8.5, 9.9); 1230 (10), 1229 (12), 1228 (12), 1227 (12), 1204 (12), 1203 (13), 1201 (18, $[M - Cl - i\text{-}Pr]^+$), 1200 (14), 1199 (15), 1198 (10), 1197 (11), 1041 (11), 1040 (13), 1038 (11), 1028 (11), 1027 (11), 1026 (14), 1025 (12), 1024 (13), 909 (15), 908 (10), 907 (15), 905 (11), 891 (11), 889 (14), 887 (17), 833 (13), 832 (14), 831 (25), 830 (15), 829 (28), 828 (12), 827 (24), 437 (15), 436 (15), 435 (13), 373 (14), 351 (14), 349 (18), 202 (15), 201 (10), 77 (16), 69 (23), 57 (53), 55 (16). Anal. calc. for $C_{66}H_{93}ClN_6O_9Zn_2$: C 61.90, H 7.32, N 6.56; found: C 61.81, H 7.28, N 6.38.

An NMR sample of **8a** in CD_3CN was allowed to stand at r.t. for several days in a vial sealed with a serum stopper leading to colorless prisms which were suitable for X-ray structure determination.

*Tris{μ-{4-(*tert*-butyl)-2,6-{bis[(4S)-4,5-dihydro-4-isopropyloxazol-2-yl]-1κN³,2κN³}phenolato-1:2κ²O}}dinickel(II) Chloride* (**8b**). As described for **8a**, from 7 (100 mg; 0.25 mmol) and $NiCl_2 \cdot 6\,H_2O$ (40 mg, 0.17 mmol): 29 mg of pale-green needles and 10 mg of dark-green prisms (total yield: 36%).

Needles **8b**: M.p. > 300°. $[\alpha]_D = +853.9$ ($c = 0.08$, $CHCl_3$). UV ($CHCl_3$): 695 (37), 378 (27800). IR (KBr): 3423*m* (br.), 2962*s*, 2904*m*, 2870*m*, 1630*s*, 1594*m*, 1573*s*, 1467*m*, 1392*w*, 1367*m*, 1329*w*, 1299*w*, 1266*m*, 1249*m*, 1219*s*, 1190*s*, 1085*m*, 1050*w*, 1004*m*, 977*m*, 845*m*, 794*m*, 742*m*, 613*m*, 487*w*. FAB-MS (NBA): isotope cluster for $[Ni_2L_3]^+$ (obs., calc.): 1237 (1.7, 1.7), 1236 (3.7, 3.9), 1235 (15.8, 16.2), 1234 (25.4, 26.9), 1233 (48.4, 49.8), 1232

(65.2, 66.5), 1231 (99.8, 100), 1230 (78.8, 72.0), 1229 (100, 92.4); cluster for $[Ni_2L_2]^+$: 866 (1.5, 1.2), 865 (2.7, 2.4), 864 (6.5, 6.5), 863 (9.4, 9.8), 862 (21.5, 22.4), 861 (25.4, 26.4), 860 (50.3, 53.5), 859 (33.4, 30.5), 858 (61.3, 58.9). Anal. calc. for $C_{66}H_{93}ClN_6Ni_2O_9$: C 62.55, H 7.40, N 6.63; found: C 62.35, H 7.42, N 6.47.

Prisms **8b**: M.p. > 300°. $[\alpha]_D$ = + 740 (c = 0.12, $CHCl_3$). FAB-MS (NBA): isotope cluster for $[Ni_2L_3]^+$ (obs., calc.): 1237 (1.7, 1.7), 1236 (3.7, 3.9), 1235 (15.8, 15.2), 1234 (25.4, 25.3), 1233 (48.4, 47.2), 1232 (65.2, 65.0), 1231 (99.8, 98.1), 1230 (78.8, 77.5), 1229 (100, 100); cluster for $[Ni_2L_2]^+$: 866 (2.0, 1.6), 865 (3.0, 3.1), 864 (7.7, 8.4), 863 (14.4, 12.7), 862 (28.3, 28.9), 861 (31.9, 34.7), 860 (64.2, 69.0), 859 (41.7, 39.4), 858 (80.5, 76.0); 1213 (9), 1187 (12), 1025 (6), 875 (10), 844 (14), 816 (16), 430 (24, [NiL + H]$^+$). Anal. calc. for $C_{66}H_{93}ClN_6Ni_2O_9 \cdot CH_2Cl_2$: C 59.51, H 7.08, N 6.21; found: C 59.13, H 7.02, N 6.26.

*{μ-{2,6-{Bis{(4S)-4,5-dihydro-4-[(1-methyl-1*H*-imidazol-4-yl)methyl]oxazol-2-yl}-1*κN^3*,1*κN$^{3'}$*,2*κN^3*,2*κN$^{3'}$*}-3,5-dimethylphenolato* 1:2κ^2O*}}-μ-hydroxo-(μ-perchlorato-*κO:κO′*)dicopper(II) Perchlorate Dihydrate* (**15**). To a soln. of ligand **2** (200 mg, 0.22 mmol) in MeOH (10 ml), a soln. of $Cu(ClO_4)_2 \cdot 6\,H_2O$ (165 mg, 0.44 mmol) in MeOH (10 ml) was added. The resulting dark green homogeneous soln. was stirred for 30 min at r.t., filtered through cotton-wool (wad in pipette), and allowed to stand at r.t. in a glass vial sealed with a plug of cotton-wool. After 5 days, the crystalline product was collected by filtration, washed with MeOH, and dried in air yielding 95 mg (52%) of **15** as dark-blue needles. Recrystallization from MeOH/EtOH 10:1 provided dark-blue prisms which were suitable for X-ray analysis. M.p. > 300° (dec.). $[\alpha]_D$ = – 223.9 (c = 0.091, MeOH). UV (MeOH): 632 (135), 346 (9900), 248 (31200), 212 (33600). IR (KBr): 3443*m* (br.), 3143*w*, 2938*w*, 1616*s*, 1567*s*, 1532*m*, 1478*w*, 1428*m*, 1375*m*, 1360*m*, 1330*w*, 1288*w*, 1244*m*, 1216*m*, 1092*s* (br.), 1027*m*, 983*m*, 942*w*, 793*w*, 623*s*. FAB-MS (NBA): isotope cluster for $[Cu_2(ClO_4)(O)L(NBA)]^+$ (obs., calc.): 830 (5.8, 7.0), 829 (11.7, 12.9), 828 (36.8, 37.8), 827 (27.9, 30.4), 826 (82.7, 83.5), 825 (24.0, 24.3), 824 (62.8, 63.5); cluster for $[Cu_2(O)L(NBA)]^+$: 729 (3.5, 4.9), 728 (4.9, 6.4), 727 (15.4, 17.6), 726 (6.4, 6.9), 725 (18.1, 18.4); 594 (0.9), 593 (3.7), 592 (7.0), 591 (15.6), 590 (10.2), 589 (19.3), 579 (2.1), 578 (4.9), 577 (18.3), 576 (18.4), 575 (60.3), 574 (23.4), 573 (69.1, Cu_2L^+), 572 (6.1), 571 (11.7), 479 (14), 477 (15), 438 (8), 437 (30), 436 (11), 435 (37), 376 (14), 375 (11), 374 (43), 373 (15), 372 (28), 203 (22), 201 (56), 171 (49), 136 (41), 95 (100, CH_2ImMe^+), 77 (65), 63 (47). Anal. calc. for $C_{24}H_8Cl_2Cu_2N_6O_{12} \cdot 2\,H_2O$: C 34.88, H 3.90, N 10.17; found: C 34.76, H 3.34, N 10.15.

*Bis{μ-{3,6-{bis[(4S)-4-benzyl-4,5-dihydrooxazol-2-yl]-1*κN^3*,2*κN^3*}pyridazine-1*κN^1*:2*κN^2*}}tetrachlorodinickel(II) Tetrahydrate* (**21b**). To a soln. of ligand **3** (20 mg, 0.05 mmol) in MeCN (2 ml), a soln. of $NiCl_2 \cdot 6\,H_2O$ (12 mg, 0.05 mmol) in MeOH (1 ml) was added. The resulting homogenous light green soln. was stirred at r.t. for 30 min, transferred into a vial sealed with a wad of cotton-wool, and allowed to stand at r.t. for several days. The crystalline product was collected by filtration, washed with MeCN and dried *in vacuo* to afford 23 mg (79%) of **21b** as a pale yellow microcrystalline powder. Recrystallization from MeCN afforded light green prisms which were suitable for X-ray analysis. M.p. > 240° (slow dec.). $[\alpha]_D$ = – 5.0 (c = 0.11, $CHCl_3$). UV (MeOH): 274 (11000), 207 (25600). IR (KBr): 3250*s* (br.), 1656*s*, 1596*s*, 1560*w*, 1495*m*, 1473*w*, 1453*m*, 1424*m*, 1377*s*, 1325*w*, 1296*m*, 1224*w*, 1175*s*, 1105*m*, 1028*w*, 952*m*, 861*w*, 735*m*, 703*m*, 539*m*. FAB-MS (NBA): isotope cluster (obs., calc.) for $[Ni_2Cl_3L_2]^+$: 1026 (0.1, 0.6), 1025 (3.4, 3.5), 1024 (3.8, 6.1), 1023 (16.6, 16.6), 1022 (18.5, 17.2), 1021 (35.7, 35.8), 1020 (23.9, 22.2), 1019 (41.9, 42.8), 1018 (9.9, 10.3), 1017 (20.9, 20.7); cluster for $[NiCl_2L]^+$: 895 (2.3, 2.4), 894 (5.8, 6.1), 893 (15.8, 15.8), 892 (23.6, 23.9), 891 (46.2, 47.0), 890 (32.0, 30.6), 889 (54.2, 54.1); cluster for $[NiClL]^+$: 495 (3.3, 8.6), 494 (4.5, 8.8), 493 (17.3, 17.2), 491 (22.8, 22.3); cluster for $[NiL]^+$: 462 (1.1, 1.6), 461 (0.7, 1.7), 460 (2.9, 7.5), 459 (13.1, 13.1), 458 (42.7, 42.6), 457 (37.0, 28.8), 456 (100, 100); 984 (23, $[Ni_2Cl_2L_2]^+$), 854 (24), 551 (16), 364 (18), 192 (24), 117 (53), 91 (99), 77 (20), 63 (18), 51 (23). Anal. calc. for $C_{24}H_{22}Cl_2N_4O_2 \cdot 3\,H_2O$: C 49.52, H 4.85, N 9.62; found: C 49.70, H 4.56, N 9.53.

Treatment of **21b** *with Silver Trifluoromethanesulfonate.* To a soln. of **21b** (7.5 mg) in CD_3OD (0.7 ml), AgOTf (16 mg) was added, the resulting mixture refluxed for 1 min, and the precipitated AgCl removed by centrifugation. The resulting (almost colorless) soln. was used for NMR experiments without further purification. ^{1}H-NMR (CD_3OD, 300 MHz): 2.66 (t, J = 12, PhCH_2); 3.07 (dd, J = 13.2, 4.1, PhCH_2); 4.03–4.07 (m, CH); 4.56 (t, J = 8.2, CH_2O); 5.03 (t, J = 9.8, CH_2O); 7.09–7.33 (m, Ph); 8.57 (s, H–C(4), H–C(5), pyridazine). ^{13}C-NMR (CD_3OD, 75 MHz): 42.6 (PhCH_2); 69.2 (CH); 77.0 (CH_2O); 127.3 (C(4), C(5), pyridazine); 129.7, 130.2, 130.3 (Ph); 139.1 (C(1), Ph); 150.9 (C(3), C(6), pyridazine); 164.3 (C=N).

*Bis(μ-acetato-1*κO*:2*κO′*)-diaqua-{μ-{2,7-{bis{(4S)-4,5-dihydro-4-[(1-methyl-1*H*-imidazol-4-yl)methyl]oxazol-2-yl}-1*κN^3*,1*κN$^{3'}$*,2*κN^3*,2*κN$^{3'}$*}-1,8-naphthyridine}}-1*κN^1*:2*κN^8*-dinickel(II) Diperchlorate* (**22a**). To a soln. of ligand **4** (18 mg, 40 μmol) in MeOH (0.5 ml), a soln. of $Ni(OAc)_2 \cdot 4\,H_2O$ (16 mg, 80 μmol) in MeOH (1.5 ml) was added. After stirring for 15 min, aq. $NaClO_4 \cdot H_2O$ soln. (560 mg in 0.5 ml H_2O) was added. The resulting homogeneous dark-green mixture was filtered through cotton-wool (wad in pipette) into a vial, the vial sealed with a plug of cotton-wool, and the mixture allowed to stand at r.t. for several days. The crystalline product was collected by filtration, washed with H_2O, and dried in air to afford 29.5 mg (77%) of **22a** as bright green

prisms which were suitable for an X-ray structure determination. M.p. > 280° (dec.). $[\alpha]_D = +34.2$ ($c = 0.17$, MeOH). IR (KBr): 3439*m* (br.), 3132*m*, 1663*m*, 1598*m*, 1574*m*, 1532*m*, 1473*m*, 1452*m*, 1394*m*, 1382*m*, 1333*m*, 1237*w*, 1214*w*, 1176*m*, 1098*s*, 1017*m*, 935*w*, 876*w*, 837*w*, 802*w*, 739*w*, 697*w*, 622*s*. FAB-MS (NBA): isotope cluster (obs., calc.) for $[Ni_2(AcO)(ClO_4)(OH)L(NBA)]^+$: 888 (3.5, 6.2), 887 (5.1, 7.3), 886 (19.4, 18.1), 885 (13.2, 14.5), 884 (34.5, 34.5), 883 (11.2, 11.9), 882 (28.3, 29.0); cluster for $[Ni_2(AcO)_2(ClO_4)L]^+$: 795 (2.8, 4.8), 794 (3, 5.3), 793 (13.6, 14.6), 792 (9.3, 10.5), 791 (28.6, 28.6), 790 (9.1, 8.6), 789 (27.6, 24.6); cluster for $[Ni_2(AcO)(OH)L(NBA)]^+$: 787 (8.3, 8.6), 786 (8.3, 9.2), 785 (19.3, 21.7), 784 (10.3, 10.4), 783 (25.3, 25.3); cluster for $[Ni_2(AcO)_2L]^+$: 694 (6.5, 8.3), 693 (9.9, 8.2), 692 (19.4, 21.9), 691 (12.0, 9.2), 690 (26.2, 26.2); 633 (6), 590 (14), 589 (13), 588 (15), 493 (6), 408 (8), 376 (19), 352 (10), 351 (17), 350 (20), 180 (29), 178 (15), 176 (15), 166 (11), 165 (19), 149 (27), 136 (59), 121 (22), 107 (41), 105 (18), 95 (61), 91 (17), 90 (50), 89 (97), 77 (91), 63 (59), 51 (84), 50 (56), 39 (100).

Complex **22b** *of Ligand* **4** *with* $Cu(OAc)_2 \cdot H_2O$. As described above for **22a**, from ligand **4** (40 μmol): 27 mg of **22b**. Dark-green needles. M.p. 224–226° (dec.). $[\alpha]_D = -55.8$ ($c = 0.23$, MeCN). UV (MeOH): 733 (210), 326 (9100), 243 (34600), 220 (39800). IR (KBr): 3423*s* (br.), 1678*m*, 1607*m*, 1524*m*, 1471*m*, 1447*m*, 1394*m*, 1292*m*, 1235*m*, 1205*m*, 1179*s*, 1144*s*, 1089*s*, 1016*m*, 942*m*, 924*m*, 899*m*, 832*m*, 811*m*, 787*m*, 735*m*, 636*s*, 626*s*, 581*m*, 559*m*. FAB-MS (NBA): isotope cluster for $[Cu_2(ClO_4)_2(OH)L(NBA)]^+$ (obs., calc.): 938 (2.0, 2.1), 937 (2.9, 3.2), 936 (15.7, 15.6), 935 (7.5, 7.9), 934 (26.4, 27.0), 933 (3.9, 3.7), 932 (16.5, 15.1); cluster for $[Cu_2(ClO_4)(OH)L(NBA)]^+$: 838 (3.9, 3.9), 837 (12.6, 13.2), 836 (10.5, 10.6), 835 (29.5, 29.8), 834 (8.7, 8.3), 833 (23.4, 22.7); cluster for $[Cu_2(ClO_4)_2(OH)L]^+$: 803 (6.8, 5.4), 802 (4.6, 5.5), 801 (24.3, 25.1), 800 (10.4, 11.1), 799 (43.1, 42.7), 798 (6.5, 6.2), 797 (26.0, 25.8); cluster for $[Cu_2(ClO_4)(OH)L]^+$: 703 (3.8, 5.6), 702 (14.5, 16.7), 701 (12.9, 11.7), 700 (34.9, 36.6), 699 (16.2, 9.7), 698 (30.7, 29.1); cluster for $[Cu_2(ClO_4)L]^+$: 687 (3.7, 4.3), 686 (5.7, 7.0), 685 (23.0, 23.7), 684 (17.1, 16.3), 683 (53.0, 53.9), 682 (15.2, 13.3), 681 (43.5, 42.6); cluster for $[Cu_2L]^+$: 587 (7.0, 8.4), 586 (12.4, 14.7), 585 (19.6, 15.9), 584 (38.3, 39.6), 583 (24.8, 16.8), 582 (40.4, 41.8); cluster for $[CuL]^+$: 524 (2.6, 2.2), 523 (5.0, 3.5), 522 (10.4, 11.8), 521 (34.9, 36.7), 520 (23.7, 23.3), 519 (73.2, 72.3); 718 (12), 619 (32), 599 (35), 489 (8), 451 (23), 418 (50), 381 (71), 355 (83), 298 (46), 262 (14), 218 (23), 185 (52), 145 (67), 95 (100, CH_2ImMe^+). Anal. calc. for $C_{24}H_{24}Cl_4Cu_2N_8O_{18} \cdot 4\,H_2O$: C 27.36, H 3.06, N 10.64; found: C 27.32, H 2.93, N 10.53.

UV-Spectroscopic Titrations. The concentration of the ligand soln. (50 μM) was chosen in such a way that the optical density was between 0.3 and 0.8 within the wavelength range of interest. This soln. (3 ml) was placed in a quartz UV cell, and 10-μl portions of a 100-fold more concentrated soln. of the metal salt were added. The

Table 4. *Crystallographic Data for Complexes* **8a**, **15**, *and* **22a**

	8a	**15**	**22a**
Molecular formula	$(C_{66}H_{93}ClN_6O_9Zn_2)_2$	$(C_{24}H_{30}Cl_2Cu_2N_6O_{13})_2$	$C_{29}H_{38}Cl_2N_8Ni_2O_{17}$
Me	2561.43	1617.04	958.99
Space group	$I2_13$	$P1$	$P2_12_12_1$
Z	8	1	4
a[Å]	30.7051(3)	7.706(3)	12.2939(4)
b[Å]	30.7051(3)	14.715(1)	17.1461(11)
c[Å]	30.7051(3)	14.913(1)	18.6838(9)
α[°]	90	72.796(6)	90
β[°]	90	81.437(22)	90
γ[°]	90	82.554(18)	90
V[Å^3]	28948.9(5)	1590.8(7)	3938.4(3)
D_{calc} [gcm^{-3}]	1.175	1.688	1.617
$\mu(CuK_\alpha)$ [cm^{-1}]	15.804	38.442	31.63
Scan type	$\omega/2\theta$	$\omega/2\theta$	$\omega/2\theta$
Radiation	CuK_α ($\lambda = 1.54178$)	CuK_α ($\lambda = 1.54178$)	CuK_α ($\lambda = 1.54178$)
Temperature [K]	293	293	293
2θ[°]	155.0 (2.03–77.50)	155.0 (2.32–77.49)	155 (2.17–77.50)
No. of independent refl.	5387	6733	3983
No. of refl. in refinem.	3494	5990	3524
R	0.0314	0.0531	0.0566
R_w	0.0360	0.0627	0.0617

concentration of the metal-salt soln. was chosen in such a way that 10 µl contained 1 mol-equiv. No extinction correction was applied.

NMR-Spectroscopic Titrations of a Ligand Solution with Zinc Dichloride in CD_3CN. The ligand (8 mg ± 0.1 mg) was placed in a vial and an appropriate amount (0.5–6 equiv.) of $ZnCl_2$ (from stock soln.) added. The resulting mixture was diluted up to 0.7 ml with CD_3CN, shaken vigorously, and filtered through cotton-wool (wad in pipette) into the NMR tube.

X-Ray Structure Analysis. Crystal data and parameters of the data collection are compiled in *Table 4*. Unit-cell parameters were determined by accurate centering of 25 strong independent reflections by the least-square method. Reflection intensities were collected at r.t. on a *CAD4* diffractometer. The usual corrections were applied. To avoid decomposition during data collection of complex **15**, the crystal was sealed in a capillary surrounded by its mother liquid. Diffraction absorption direct-method strategies were applied using the programs SHELXS-86 [14a] and SIR92 [14b]. Anisotropic least-squares refinement was carried out on all non-H-atoms using the program CRYSTALS [15]. Positions of H-atoms were calculated. Fractional coordinates are deposited in the *Cambridge Crystallographic Data Base*.

REFERENCES

[1] C. J. Fahrni, A. Pfaltz, *Helv. Chim. Acta* **1998**, *81*, 491.
[2] H. Adams, N. A. Bailey, P. Bertrand, C. O. Rodriguez de Barbarin, D. E. Fenton, S. Gou, *J. Chem. Soc., Dalton Trans.* **1995**, 275.
[3] C.-T. Chen, W.-K. Chang, S.-C. Sheu, G.-H. Lee, T.-I. Ho, Y.-C. Lin, Y. Wang, *J. Chem. Soc., Dalton Trans.* **1991**, 1569.
[4] E. Kimura, I. Nakamura, T. Koike, M. Shionaya, Y. Kodama, T. Ikeda, M. Shiro, *J. Am. Chem. Soc.* **1994**, *116*, 4764.
[5] N. N. Murthy, K. D. Karlin, *J. Chem. Soc., Chem. Commun.* **1993**, 1236.
[6] P. Chaudhuri, C. Stockheim, K. Wieghardt, W. Deck, R. Gregorzik, H. Vahrenkamp, B. Nuber, J. Weiss, *Inorg. Chem.* **1992**, *31*, 1451.
[7] C. Bazzicalupi, A. Bencini, A. Bianchi, V. Fusi, L. Mazzanti, P. Paoletti, B. Valtancoli, *Inorg. Chem.* **1995**, *34*, 3003.
[8] C. J. O'Connor, D. Firmin, A. K. Pant, B. R. Babu, E. D. Stevens, *Inorg. Chem.* **1986**, *25*, 2300.
[9] O. J. Gelling, A. Meetsma, B. L. Feringa, *Inorg. Chem.* **1990**, *29*, 2816.
[10] M. Maekawa, S. Kitagawa, M. Munakata, H. Masuda, *Inorg. Chem.* **1989**, *28*, 1904.
[11] T. Mallah, M.-L. Boillot, O. Kahn, J. Gouteron, S. Jeannin, Y. Jeannin, *Inorg. Chem.* **1986**, *25*, 3058.
[12] See, *e.g.*, L. Rosenberg, L. K. Thompson, E. J. Gabe, F. L. Lee, *J. Chem. Soc., Dalton Trans.* **1986**, 625, and refs. cit. therein.
[13] B. J. Hathaway, A. E. Underhill, *J. Chem. Soc.* **1961**, 3091.
[14] a) G. M. Sheldrick, 'SHELXS-86', Universität Göttingen, 1986; b) A. Altomare, G. Cascarano, G. Giacovazzo, A. Guagliardi, M. C. Burla, G. Polidori, M. Camalli, *J. Appl. Crystallogr.* **1994**, *27*, 435.
[15] D. Watkin, 'CRYSTALS, Issue 9', Chemical Crystallography Laboratory, Oxford, 1990.

Received September 15, 1997